Anti-melanoma potential of inclusion complexes containing phyllacanthone in β-cyclodextrin and sulfobutyl-ether-β-cyclodextrin

Cristiane dos Santos Cerqueira Alves, Yuri Kelvin Silva Camacho Tavares, Guilherme Urias Menezes Novaes, Victória Laysna dos Anjos Santos, Ana Paula de Oliveira, Cintia Emi Yanaguibashi Leal, Edilson Beserra de Alencar Filho, Christiane Adrielly Alves Ferraz, Laurent Picot, Jackson Roberto Guedes da Silva Almeida, et al.

Anti-melanoma potential of inclusion complexes containing phyllacanthone in β-cyclodextrin and sulfobutyl-ether-β-cyclodextrin

Cristiane dos Santos Cerqueira Alves[1], Yuri Kelvin Silva Camacho Tavares[1], Guilherme Urias Menezes Novaes[1], Victória Laysna dos Anjos Santos[1], Ana Paula de Oliveira[1,5], Cintia Emi Yanaguibashi Leal[2], Edilson Beserra de Alencar Filho[2,5], Christiane Adrielly Alves Ferraz[4,5], Laurent Picot[3,5], Jackson Roberto Guedes da Silva Almeida[1,5*], Raimundo Gonçalves de Oliveira Júnior[4,5*]

[1] Center for Studies and Research of Medicinal Plants, Federal University of San Francisco Valley, 56304-205, Petrolina, Pernambuco, Brazil

[2] Department of Pharmacy, Federal University of San Francisco Valley, 56304-205, Petrolina, Pernambuco, Brazil

[3] LIENSs UMR CNRS 7266, La Rochelle Université, 17042, La Rochelle, France

[4] UMR CNRS 8038 CiTCoM, Université Paris Cité, 75006, Paris, France. France

[5] Franco-Brazilian Network on Natural Products (FB2NP).

[*]Both authors contributed equally to the supervision of this work. Corresponding author: raimundo.goncalves-de-oliveira-junior@u-paris.fr (RGOJ)

ABSTRACT

The *bis-nor*-diterpene phyllacanthone (PHY) was isolated from the chloroform fraction of the stem barks from *Cnidoscolus quercifolius* Pohl (Euphorbiaceae). PHY/β-CD and in PHY/SB-E-β-CD inclusion complexes were obtained and characterized using NMR, SEM and FT-IR techniques. *In silico* approach show that most stable conformations presenting binding energies of -89.8068 Kcal/mol (PHY/β-CD) and -87.4032 Kcal/mol (PHY/SB-E-β-CD), corroborating FTIR and ^{1}H NMR results. The *in vitro* dissolution assay demonstrated a fast PHY release from both complexes, indicating that the complexation improved its solubility. PHY/β-CD and PHY/SB-E-β-CD inclusion complexes presented high entrapment efficiency rates (89.60% and 77.56%, respectively). PHY, PHY/β-CD and PHY/SB-E-β-CD inclusion complexes induced growth inhibition in A2058 melanoma cells when compared to the control group, suggesting that both (natural or chemically modified) CDs can be used as carriers of PHY in pharmaceutical formulations or drug delivery systems as a strategy to improve its stability and ensure better bioavailability.

Keywords: diterpene, *Cnidoscolus*, cyclodextrin, skin cancer, polymer

Highlights

- New inclusion complexes containing phyllacanthone in β-CD and SB-E-β-CD were prepared and characterized.
- Complexation with natural and chemically modified CDs improved phyllacanthone aqueous solubility.
- Inclusion complexes preserved phyllacanthone cytotoxic activity on chemoresistant melanoma cells.
- Phyllacanthone, complexed or not with cyclodextrins, mitigates the growth of A2058 melanoma cells

1. Introduction

Phyllacanthone (PHY) is a bis-*nor*-diterpene previously isolated from the stem barks of *Cnidoscolus quercifolius* Pohl (Euphorbiaceae), a Brazilian medicinal plant popularly known as "favela" or "faveleira" (Oliveira-Júnior et al., 2018). It is a species with thick leaves, tuberous roots, and small white flowers, widely disseminated in the Caatinga biome and traditionally used for the treatment of infections, tumors, and inflammation (Santos; Silva; Silva, 2020; Sobrinho et al., 2012). Previous reports have demonstrated that stem barks of "favela" are rich in cytotoxic diterpenes. Known as favelines, these molecules bear a tricyclic benzylcycloheptene skeleton (C_6-C_7-C_6) and are of unique occurrence in the genus *Cnidoscolus*. A recent study showed that PHY, majorly found in *C. quercifolius*, induces growth inhibition, cell cycle arrest, and tubulin depolymerization-mediated apoptosis in BRAF-mutated melanoma cells (Oliveira-Júnior et al., 2022).

As well as other aromatic diterpenes, PHY has high volatility and low solubility in water, which limits its pharmaceutical development. In an attempt to overcome these barriers, several carriers can be used to improve the physicochemical properties of this type of compound, and then contribute to better bioavailability (Abril-Sanchez et al., 2019). In the past decades, the use of cyclodextrins (CDs) has proven to be an effective strategy to enhance aqueous solubility and then better dissolution rates and bioavailability of non-polar anticancer drugs candidates (Gandhi et al., 2020; Carneiro et al., 2019).

CDs are macrocyclic and non-toxic oligosaccharides, usually formed by *D*-glucose units linked by $\alpha_{1\text{-}4}$ glycosidic bonds. They are often represented as one cone truncated with a hydrophilic surface and a hydrophobic central cavity, capable to host hydrophobic molecules

with low solubility in water. They confer chemical and physical stability to small molecules and their complexation in CDs' internal portion makes them ideal for solubilizing compounds in aqueous systems due to their surface polarity, forming inclusion complexes that can improve bioavailability, thermal stability (e.g. reducing evaporation losses) and also plasma stability, protecting the guest compound from enzymatic degradation after oral administration (Marques, 2010; Oliveira-Filho, 2018).

In addition to natural CDs (e.g. α-CD, β-CD and γ-CD), that differ in the number of *D*-glucose units and volume of the internal cavity, new chemically modified structures, such as hydroxypropyl-β-cyclodextrin (HP-β-CD), methyl-β-cyclodextrin (M-β-CD) and sulfobutyl-ether-β-cyclodextrin (SB-E-β-CD) were synthesized to improve the complexing properties. In fact, the solubility and complexing capacity of natural CDs are limited and could not be applicable to several compounds. Chemical modifications can be planned to overcome these limitations and to enhance CDs' ability to form inclusion complexes (Brewster; Loftsson, 2007). For example, electrostatic attraction between the positive charge of the guest and the negative charge of the SB-E-β-CD increases the effect of host-guest complexation and enhances solubility (Fenyvesi et al., 2014).

The present work sought to obtain and characterize the formation of inclusion complexes containing phyllacanthone isolated from stem barks of *Cnidoscolus quercifolius* in β-cyclodextrin and evaluate the effect of complexation on the cytotoxic activity of the bis-*nor*-diterpene in human melanoma cells. In order to compare their complexation performance, inclusion complex using sulfobutyl-ether-β-cyclodextrin was also developed and tested.

2. Materials and methods

2.1. Drugs and chemicals

Phyllacanthone (PHY, >99%) was isolated from *C. quercifolius* stem-barks as described bellow. β-CD (>99%) was purchased from Sigma-Aldrich® and SB-E-β-CD (Dexolve®, >99%) was kindly provided by Cyclolab (Brazil). Organic solvents (ethanol, chloroform, hexane and methanol) were purchased from Synth® lab (Brazil).

2.2. Plant material

Stem barks of *Cnidoscolus quercifolius* Pohl were collected in Petrolina-PE, in a Caatinga zone from the Federal University of Vale do São Francisco (UNIVASF) (09°19'43"

S / 40°33'09" W). The plant material was previously identified by a botanist, and a comparison was made with a specimen already deposited (voucher #19202) in the Herbarium Vale do São Francisco (HVASF) of UNIVASF, being registered in the National System for Managing Genetic Heritage and Associated Traditional Knowledge (SisGen), under the record number AB179D2. The plant material was then dried in an oven with air circulation (40 °C, for 72 hours) and pulverized, yielding 900 g of stem barks powder.

2.3. Extraction and purification of phyllacanthone (PHY)

PHY was extracted and purified as previously described (Oliveira-Júnior et al., 2018). Dried and pulverized plant material was subjected to an exhaustive maceration using ethanol 95% as solvent. The extractive solution was filtered and concentrated in a rotary evaporator, yielding 61 g of ethanol extract. Part of the extract (30 g) was fractioned by vacuum liquid chromatography (VLC), using silica gel 60 as stationary phase. Hexane, chloroform, ethyl acetate, and methanol were used as mobile phase, in increasing order of polarity, resulting in the respective fractions.

Chloroform fraction (6 g, from which PHY was previously isolated) was applied on preparative TLC plates (silica gel 60, 2-25 µm, Merk®) and eluted with hexane/ethyl acetate (97:3). The entire process was monitored with a UV flashlight and a sub-fraction containing 700 mg of purified PHY was obtained and then analyzed by 1D and 2D NMR for structural characterization.

2.4. Obtention of inclusion complexes

Inclusion complexes of PHY in β-CD (Sigma-Aldrich®) and in SB-E-β-CD (Dexolve®, Cyclolab) were prepared in a 1:1 molar ratio (100 mg of PHY to 0.998 g of β-CD and 100 mg of PHY to 1.970 g of SB-E-β-CD). A solution of 75% water and 25% ethanol was added to the mixture, for a total of 250 mL of solution. The used amount of PHY was added to the used volume of ethanol, and the mixture was subjected to ultrasound (10 minutes at 25 °C). The water solutions and the respective CDs were added to the mixtures and placed in a magnetic stirrer for 48 h. PHY/β-CD solution was lyophilized, while PHY/SB-E-β-CD solution was left in an oven with circulating air (at 45 °C) in a glass container for 48 hours. Physical mixtures were prepared in the same molar ratio, ground, and stored in a freezer until future analyses (Alves et al., 2019).

2.5. Scanning electron microscopy (SEM)

Surfaces of PHY, CDs, physical mixtures, and inclusion complexes were examined in a scanning electron microscope model TescanVEGA3. Samples were prepared by mounting the powders on carbon tape placed under aluminum foil. Subsequently, the powders were metalized with gold powder for 12 minutes and examined using SEM at 10 kV.

2.6. Fourier transform infrared (FTIR)

FTIR spectra were obtained using KBr pellets as solid support. To prepare the tablets, approximately 1 mg of the sample was used for 100 mg of KBr, which were macerated until a fine powder was obtained. The mixture was then subjected to a pressure of 78.5 KN, using a Shimadzu® hydraulic press for a period of ten minutes. The samples were then analyzed in an IRTracer-100 spectrometer, Shimadzu®, in the region between 4000 and 400 cm^{-1}, with 45 scans and a resolution of 8 cm^{-1}.

2.7. Nuclear magnetic resonance (NMR)

1D and 2D ^{1}H NMR experiments were acquired using D_2O and conducted in a Bruker™ 400 MHz ASCEND III spectrometer, operating at 9.4 Tesla, equipped with a 5 mm direct detection probe and *z*-axis field gradient. ^{1}H NMR chemical shifts were expressed relative to the TMS signal at δ 0.00 (reference compound) and coupling constants (*J*) were expressed in Hz.

2.8. In silico procedures

Initially, a molecular docking analysis was performed using Autodock Vina (Trott and Olson, 2010) program and Autodock Tools (Morris et al., 2009) graphical interface, only to generate an initial pool of conformations for further semi-empirical refinement. The structure of βCD was taken from the RCSB-PDB crystallographic database (www.rcsb.org) PDB ID: 5MK9. The structure of SB-E-β-CD was drawn from the three-dimensional structure of 5MK9 in Chemsketch, following the sulfonation pattern of the inclusion complex used experimentally. Chimera software (Pettersen et al., 2004) was used to add hydrogens. The 3D structure of PHY was obtained from PubChem (www.pubchem.ncbi.nlm.nih.gov), with hydrogens added also with Chimera software. For Vina calculations, the dimensions of gridbox were 14 x 13 x 13 Å and 21 x 21 x 21 Å with a default spacing of 1.0 Å between the grid points, centered on β-CD and SB-E-β-CD, respectively. Starting from the best poses found in Vina, semi-empirical calculations were performed using PM6-DH2 Hamiltonian with the MOPAC2016 package (Stewart, 2016). The final binding energies after semi-

empirical calculations (ΔE), considering the heat of formation (ΔH° f) of each system, were evaluated as:

$$\Delta E = \Delta H^\circ f_{(complex)} - [\Delta H^\circ f_{(host)} + \Delta H^\circ f_{(guest)}]$$

2.9. Entrapment efficiency

The real concentration of PHY complexed into CDs was determined using a protocol previously described (Ferraz et al., 2020). Firstly, the superficially adsorbed PHY was removed from both complexes (PHY/β-CD and PHY/SB-E-βCD) by washing 10 mg of the sample with 10 mL of ethanol for 10 minutes with stirring. The resulting solution was centrifuged at 4500 g for 5 min (25 °C) in order to remove any remaining CD. Then, the supernatant containing the adsorbed PHY was collected and filtered through a membrane filter (0.22 μm filter, Millipore™). An aliquot (1000 μl) of the filtrate was added to quartz cuvettes for absorbance reading in a UV-Vis spectrophotometer at 260 nm. A standard curve (30-60 μg/ml, $R^2 = 0.9911$) was constructed under the same conditions to calculate the final PHY concentration (n=3). Finally, the entrapment efficiency (EE%) was calculated according to the equation:

$$EE\% = (\text{mass of PHY recovered} / \text{mass of PHY in the complex}) \times 100$$

2.10. In vitro dissolution test

A dissolution profile of PHY and its inclusion complexes was performed as previously proposed (Oliveira et al., 2019). Initially, the maximum wavelength of PHY was determined by scanning at wavelengths of 200-400 nm in saline solution (0.15 M) acidified to pH 1.5 with hydrochloric acid (37 ºC) using a UV-Vis spectrophotometer. A calibration curve was performed using concentrations between 2-30 $\mu g.mL^{-1}$ ($Y = 0.0033X + 0.0077$, $R^2 = 0.9911$, where X is the PHY concentration and Y is the absorbance at 260 nm at 37 °C).

For the controlled release study, free PHY and its inclusion complexes were placed in 50 mL of saline solution, and the experiments were carried out in a magnetic stirrer with controlled temperature and agitation (37 ºC and 100 rpm, respectively) for a total time of 100 minutes. At periodic intervals, samples of the release medium were taken and analyzed by spectrophotometry at 260 nm to determine the amount of released PHY. Results were obtained from three independent experiments.

2.11. Evaluation of cytotoxic activity

The cytotoxic activity was determined by the MTT method, described by Mossman (1983) and adapted by Oliveira-Júnior (2022). Samples were solubilized in DMSO (dimethylsulfoxide) and diluted in the culture medium (final DMSO concentration < 1%, used as control). A2058 melanoma cells (2 x 10^3 cells/well) were exposed to PHY and its inclusion complexes at the same concentration (50 µM) for 72 h. CDs and physical mixtures were also tested under the same conditions. After the incubation period, cell morphology was evaluated under an inverted phase contrast microscope (Nikon, Eclipse, France) and a MTT solution (5 g/L) was then added to each well. Formed formazan crystals were solubilized in 200 µL of DMSO and absorbance readings were performed at 550 nm, using the FLUOstar Omega microplate reader (BMG Labtech®, France). The percentage of cell growth inhibition (GI%) was then calculated using the following equation:

$$GI\% = 100 - [(Aa - Ab) / (Ac - Ab)] \times 100$$

Where: Aa represents the absorbance of the wells containing cells treated with the samples; Ab represents the absorbance of empty wells (blank) and Ac represents the absorbance of wells containing only cells grown in culture medium + final DMSO concentration. Results were obtained from at least three independent experiments.

2.12. Statistical analysis

Statistical analysis was performed using one-way analysis of variance (*one-way* ANOVA*)* followed by Tukey's multiple comparison test. *P* values < 0.05 were considered statistically significant. All analyzes were performed using GraphPad software Prism® 5.0 (GraphPad Prism Software, Inc., San Diego, CA, USA).

3. Results and discussion

3.1. SEM analysis

SEM analysis can visually demonstrate the morphological difference between isolated and complexed compounds, and morphological modifications can be assumed as proof of the formation of a solid inclusion complex with a CD's hydrophobic cavity (Srinivasan; Stalin, 2014). The results of SEM analyses for PHY, β-CD, SB-E-β-CD, physical mixtures, and inclusion complexes are shown in Figure 1.

PHY exhibited plane-shaped crystals, while SB-E-β-CD has a spherical structure and β-CD has a very characteristic morphology, resembling large rectangles. Physical mixtures preserved the crystalline and amorphous structures of PHY and both CDs, respectively, presenting characteristics that can be attributed to the isolated carriers and, possibly, to the PHY – thus, the compound is not inserted in the cavity of the host molecule. In fact, it is common to have preserved characteristics for both host and guest during SEM analysis of physical mixtures. In this case, CDs are often covered and/or surrounded by small crystals from the guest compound, maintaining the original morphology (Domingues et al., 2022).

However, both complexes showed alterations in CDs morphology and a reduction in the crystallinity of PHY. Inclusion complexes exhibited quite singular morphological changes, linked to a reduction in particle size and to a transformation to an amorphous structure (when compared with isolated CDs and physical mixtures).

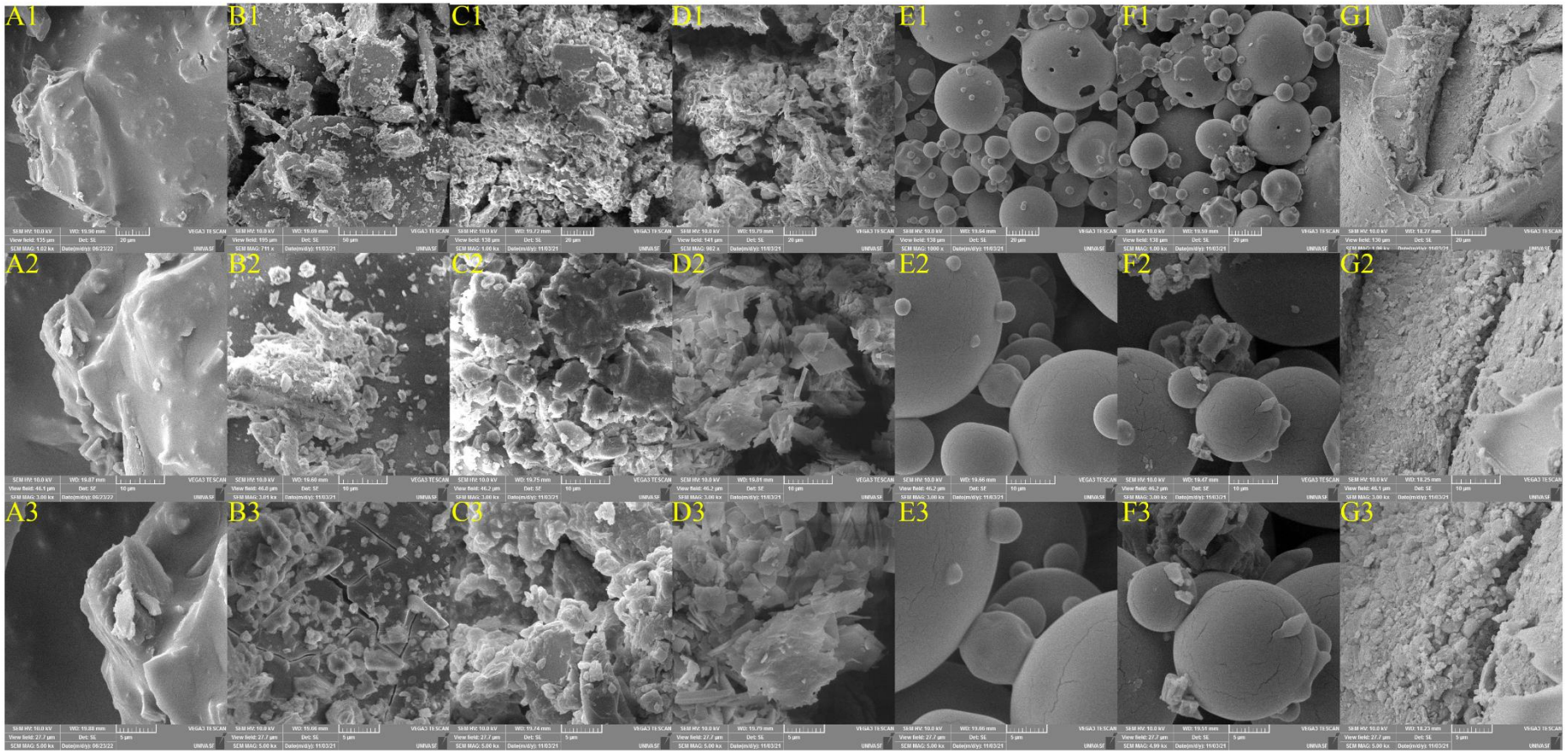

Figure 1 – Scanning Electron Microscopy of PHY (A1, A2, A3); β-CD (B1, B2, B3); physical mixture of PHY/β-CD (C1, C2, C3); PHY/β-CD inclusion complex (D1, D2, D3); SB-E-β-CD (E1, E2,E3); physical mixture of PHY/SB-E-β-CD (F1, F2, F3); PHY/SB-E-β-CD inclusion complex (G1, G2, G3). Magnifications of 1000x, 3000x, and 5000x, respectively.

3.2 FTIR analysis

FTIR is a useful tool for the characterization of vibrational patterns because it is able to show changes in characteristic bands of CDs, such as broadening, narrowing, disappearance, or change in intensity, which may be indicative of the formation of inclusion complexes (Mura, 2015). FTIR spectra of PHY, CDs, inclusion complexes, and physical mixtures are shown in Figure 2.

Analyses of PHY/β-CD and PHY/SB-E-β-CD inclusion complexes spectra show a reduction in the intensity of the characteristic bands of PHY. Absorption bands are clearly noted in the region of 3000 cm^{-1} (O-H stretching), 2900 cm^{-1} (C-H stretching), at 1154 cm^{-1} (C-O stretching) and 1026 cm^{-1} (C-O-C stretching), all characteristic of β-CD and SB-E-β-CD, with a slight displacement of the O-H and C-H stretching bands. This finding suggests that PHY, in both complexes, is interacting more strongly with the CDs' cavity, resulting in greater conformational restriction, reducing the free movement of the included molecules and then decreasing the intensity of the signal (Eid et al., 2011). This absorption pattern is not observed in the physical mixtures spectra, which is not as deformed as in the absorption pattern of inclusion complexes.

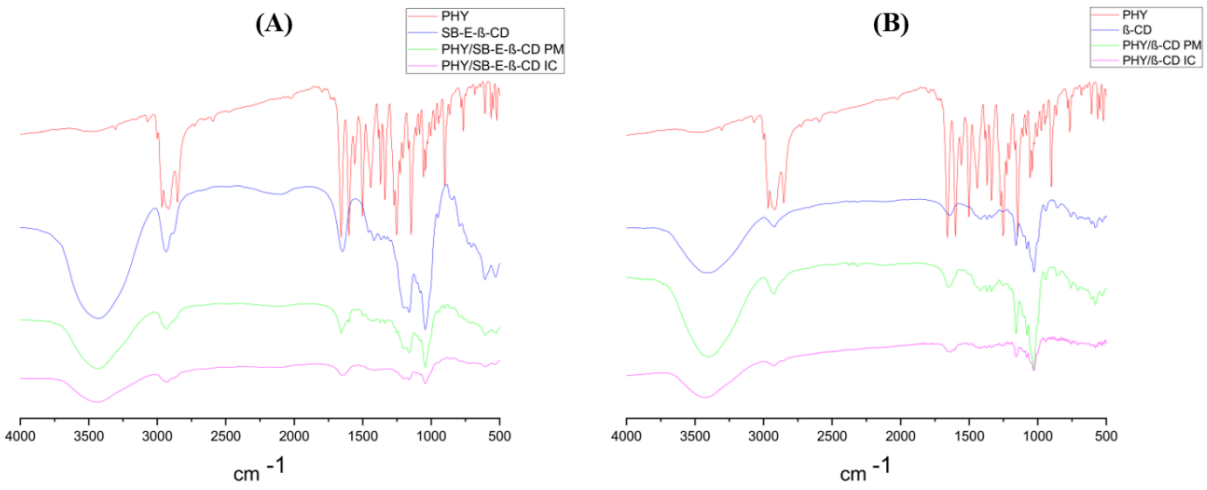

Figure 2 - FTIR characterization for (A) – PHY (red), β-CD (blue), PHY/β-CD physical mixture (PM, green), PHY/β-CD inclusion complex (IC, pink); and (B) – PHY (red), SB-E-β-CD (blue), PHY/SB-E-β-CD physical mixture (PM, green), PHY/SB-E-β-CD inclusion complex (IC, pink).

3.3 NMR analysis

The interaction of CDs with an encapsulated compound during formation of an inclusion complex can be demonstrated by spectral variations through changes in chemical shifts, mainly through variations of internal hydrogens (Bernini et al., 2004). Thus, the formation of inclusion complexes was observed based on the chemical shifts of the CDs protons that remain inside the cavity, hydrogen 3 (H-3) and hydrogen 5 (H-5), which will be altered once the guest molecule is inside of it (Jahed et al., 2014). Chemical shifts are shown in Table 1 and ^{1}H NMR spectra are presented in Figure 3.

The experiment for PHY/β-CD and PHY/SB-E-β-CD inclusion complexes showed that internal hydrogens (H-3, H-5, and H-6) were shifted in a lower frequency region, indicating that they were shielded in the presence of the guest molecule. To confirm this mode of complexation, ^{1}H-^{1}H ROESY NMR experiment was carried out, since it is considered one of the most effective techniques to study the internal interactions of host-guest in inclusion complexes (Ali; Muzzafar, 2019). However, no correlations between the hydrogens of the molecules were observed, probably due to overlapping signals. To determine the most stable poses of the inclusion complexes, considering a gap of ^{1}H-^{1}H ROESY information, an *in silico* study can be assigned (Oliveira et al., 2019).

Table 1 - ^{1}H NMR, chemical shifts (δ, ppm) in D_2O of β-CD/SB-E-β-CD and changes observed for the inclusion complexes (PHY/β-CD and PHY/SB-E-β-CD).

Proton	**β-CD**	**PHY/β-CD**	**Δδ**
H-2	3.6104	3.6099	0.0005
H-3	3.9918	3.9907	0.0011
H-4	3.6760	3.6754	0.0006
H-5	3.8806	3.8782	0.0024
H-6	3.9045	3.9033	0.0012
Proton	**SB-E-β-C**	**PHY/SB-E-β-CD**	**Δδ**
H-2	3.6348	3.6340	0.0008
H-3	4.0650	4.0625	0.0022
H-4	3.6499	3.6495	0.0004

H-5	3.9088	3.9081	0.0007
H-6	3.8438	3.8407	0.0031

$\Delta\delta = \delta_{CD} - \delta_{inclusion\ complex}$ (positive or negative values). Data obtained from Bruker Avance III 400 MHz. The most significant Δδ were observed for H-3, H-5 and H-6.

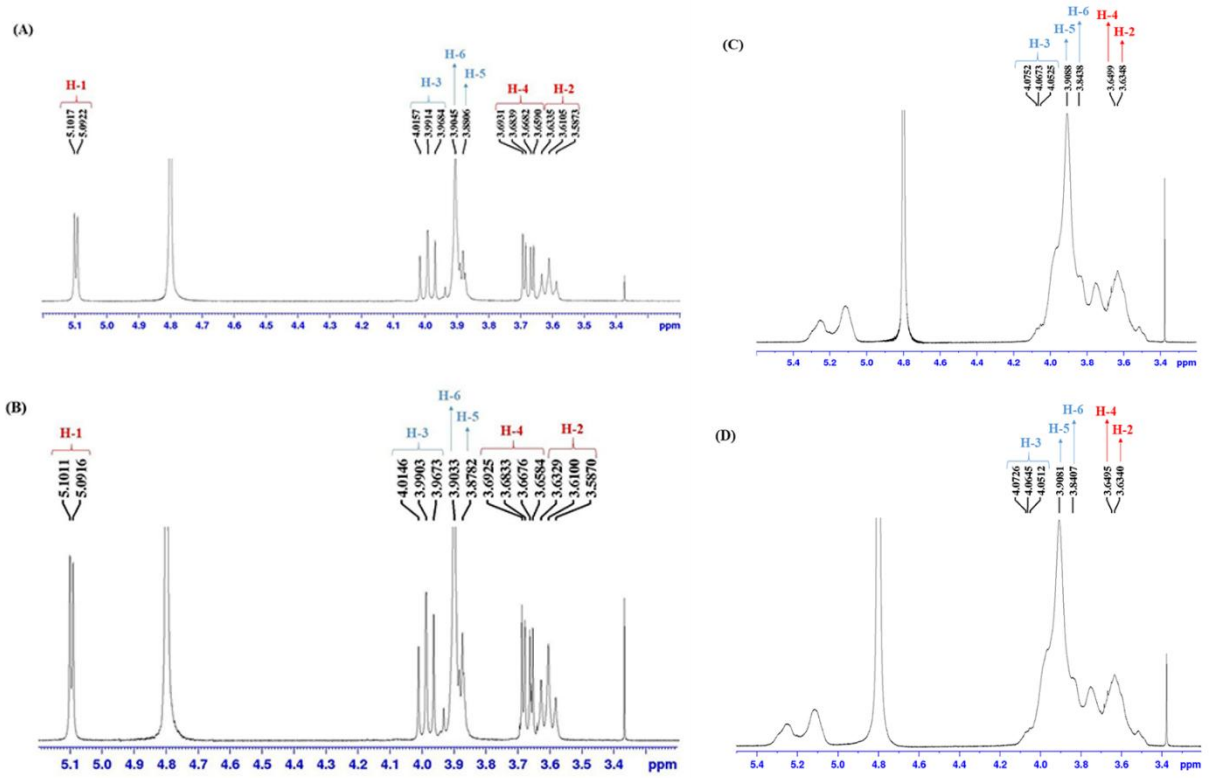

Figure 3 - ^{1}H NMR spectra obtained for β-CD (A), PHY/β-CD (B), SB-E-β-CD (C) and PHY/SB-E-β-CD (D) in D_2O.

3.4 In silico procedures

To confirm and better understand the complexation mode of PHY into the CDs' internal cavity, molecular docking studies were applied to characterize the three-dimensional structure of inclusion complexes, based on the binding energies. During PH6-DH2 calculations, it is established that lower energy values indicate better guest/host interaction (Sapte; Pore, 2016).

The conducted molecular docking studies of PHY/β-CD PHY/SB-E-β-CD inclusion complexes help understand the binding affinity and stability of the interactions. Data predicted that β-CD and SB-E-β-CD can encapsulate PHY within their hydrophobic cavity, and PM6-DH2 calculations suggested that the most stable conformations (Figure 4) show

binding energies of -89.8068 Kcal/mol (PHY/β-CD inclusion complex) and -87.4032 Kcal/mol (PHY/SB-E-β-CD inclusion complex).

Properties such as size, charge and polarity of the molecule can influence the ability and stability of inclusion complex formation (Faucci; Melani; Mura, 2002). The results indicated that PHY was preferably inserted through the substituted benzene, corroborating FTIR and ^{1}H NMR results (absence of peaks from axial deformation attributed to a methoxyl group and more significant interaction between H-3, H-5 and H-6 with a possible guest molecule). Based on this findings, the possible inclusion mode of PHY in both β-CD and SB-E-β-CD cavities is presented in Figure 5.

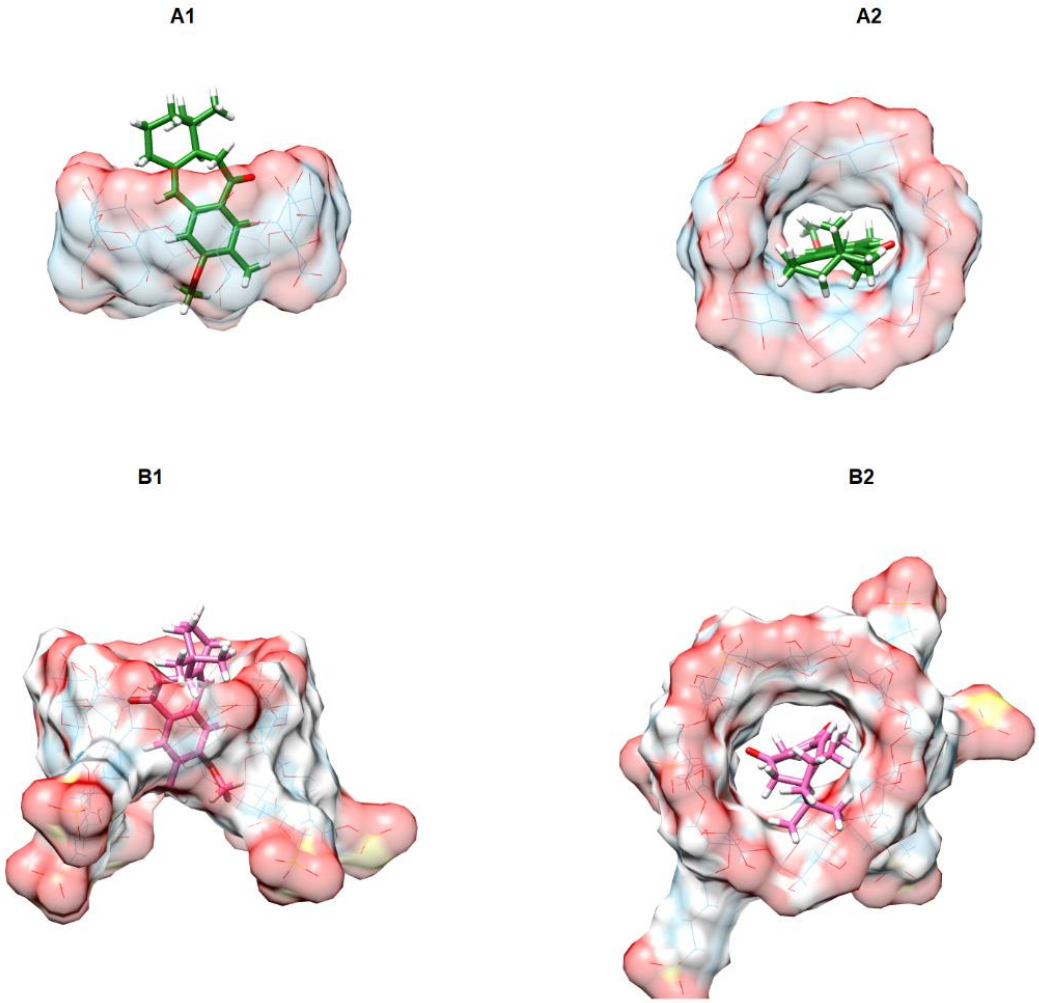

Figure 4 – Most stable docking conformations for PHY/β-CD (A1/A2) and PHY/SB-E-β-CD (B1/B2) in two visualization modes.

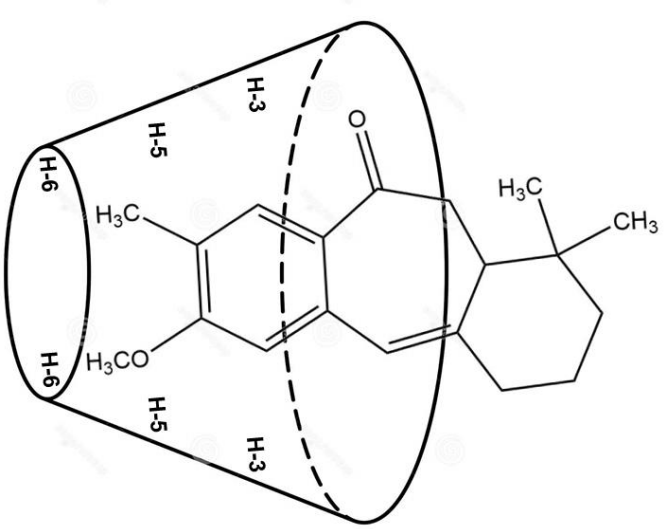

Figure 5 - Possible inclusion mode of PHY in the internal cavity of β-CD and SB-E-β-CD.

3.5 In vitro dissolution test

CDs are widely used by pharmaceutical industries for various purposes, including improvement of thermal and plasma stability, as well as enhancement of aqueous solubility, since most drug candidates are hydrophobic. Considering the low solubility of PHY as a limiting factor for its pharmaceutical development, we performed the dissolution test. In order to mimic stomach conditions, the dissolution test was carried out in pH-adjusted and temperature-controlled saline solution (pH 1.5 at 37 °C) (Oliveira et al., 2019).

As shown in Figure 6, there was no dissolution of PHY into the medium during the entire experiment time (100 minutes). However, when complexed with both CDs, PHY exhibited a high release rate in the first five minutes, especially for PHY/SB-E-βCD (>90%). After 30 min, both complexes presented a dissolution rate >95%, indicating that complexation of PHY in βCD or SB-E-βCD may significantly enhance its solubility under the tested conditions. This observation is often well associated to a greater *in vivo* bioavailability of organic compounds. An improved solubility combined with the permeation capacity intrinsic to hydrophobic molecules usually contribute to a better bioavailability (Zhou et al., 2012).

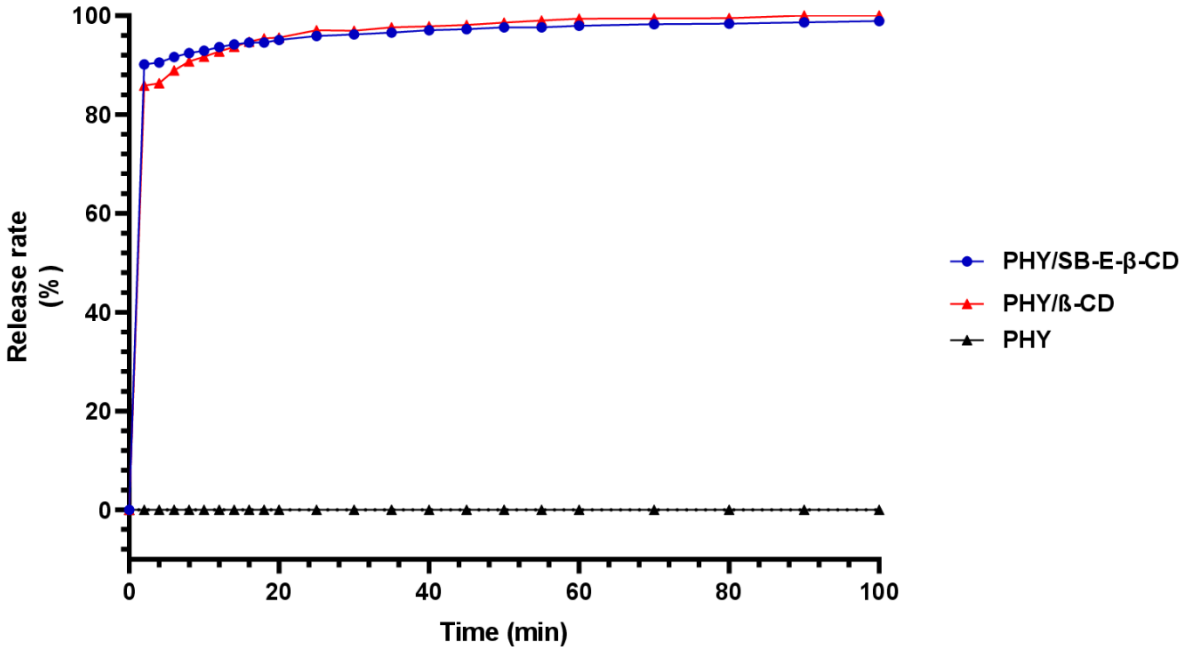

Figure 6 – Graph for the *in vitro* release rate, demonstrating the variation in the concentration of PHY in saline solution when in an inclusion complex with β-CD and SB-E-β- CD (for a total time of 100 minutes).

3.6 Entrapment efficiency

The entrapment efficiency (EE%) is a quantitative parameter used to determine the real amount of the guest molecule present in the inner cavity of the CDs. A high EE% indicates efficiency of the chosen complexation method and ensures better dissolution rate and consequently better bioavailability (Kumar et al., 2017). In the present study, the EE% obtained for PHY/β-CD and PHY/SB-E-β-CD were of 89.60% and 77.56%, respectively, representing a satisfactory complexation yield. Many factors can influence the interactions between guest molecules and CDs, including the type of cyclodextrin (which differ in the size of the cavity), the complexation method and the level of hydrophobicity of the guest molecule (Fenyvesi et al., 2016). The high encapsulation efficiency values observed for both inclusion complexes indicate that a large amount of PHY was actually inserted into the CDs internal cavity.

3.7 *Evaluation of cytotoxic activity*

Phyllacanthone is the major diterpene found in *C. quercifolius.* In a recent study, we have shown that this compound inhibits cell proliferation and migration, and induces apoptosis in chemoresistant melanoma cells by disrupting the cell cytoskeleton.

Immunoassays and molecular docking experiments revealed PHY induces tubulin depolymerization through a strong interaction with the colchicine-specific binding site (Oliveira-Junior et al., 2022). Despite its anti-melanoma potential, PHY has poor solubility, which limits its efficacy and hinders its pharmaceutical development. Its complexation in two different CDs could improve its physicochemical properties without compromising its anti-melanoma activity. This hypothesis was confirmed by testing PHY alone and complexed with both β-CD and SB-E-β-CD. As shown in Figure 7, PHY 50 µM exhibited a percentage of cell growth inhibition of 35.50 ± 4.81%. PHY/β-CD and PHY/SB-E-β-CD inclusion complexes showed a percentage of inhibition of 42.98 ± 3.70% and 39.95 ± 2.5%, respectively, both with a statistically significant difference when compared to control group (p<0.05). Microphotographs (Figure 7C) for the cytotoxic activity of PHY and inclusion complexes showed a reduction of the cell population promoted by the treatments. These findings are in accordance with previous reports by Oliveira-Júnior et al. (2022), that described the moderate concentration dependent cytotoxic potential and cell inhibition promoted by PHY against A2058 melanoma cells.

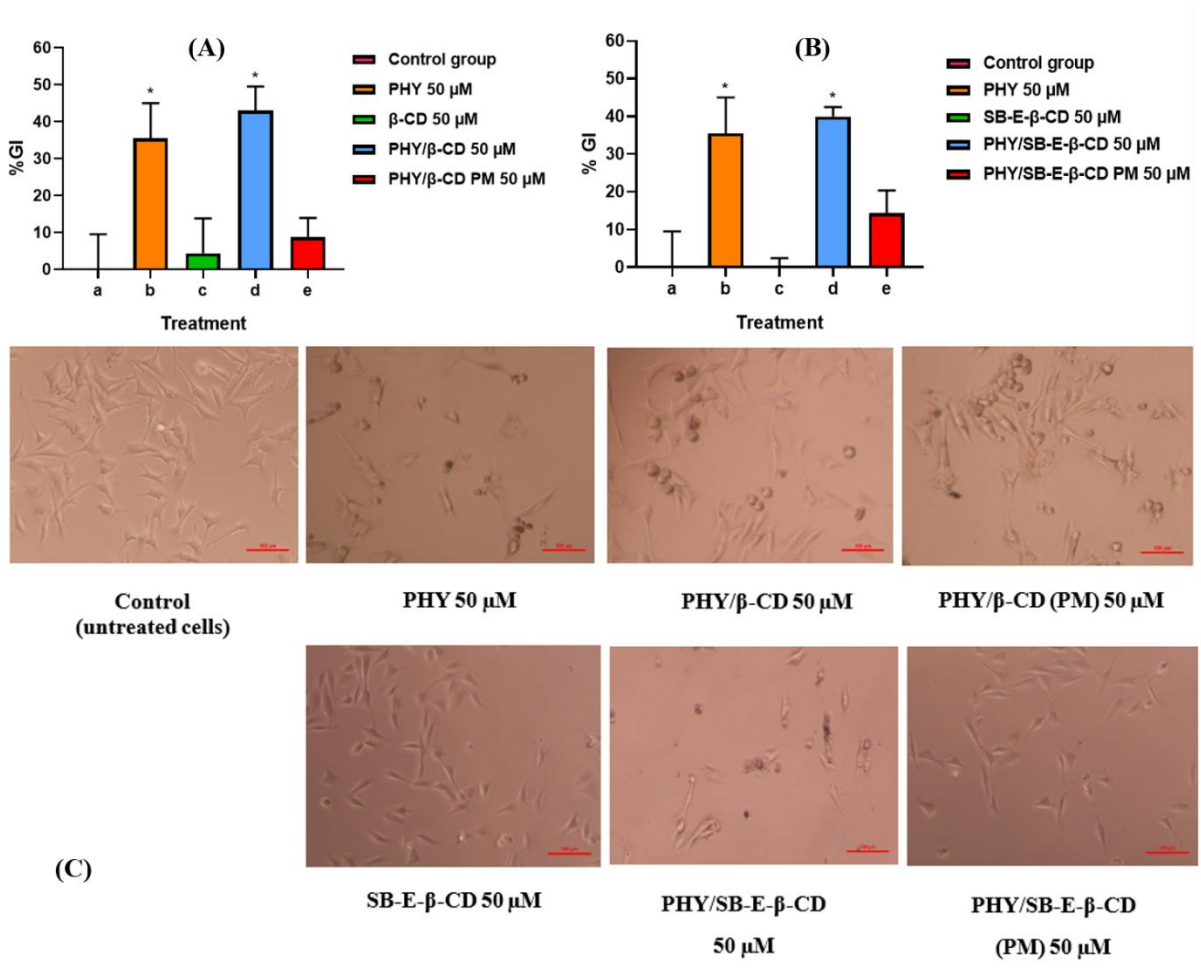

Figure 7. Cytotoxic activity of PHY (50 μM), PHY/β-CD and PHY/SB-E-β-CD inclusion complexes and physical mixtures (A and B). Data are expressed as mean of %GI (Growth Inhibition) ± SEM, *$p < 0.05$ (vs. control group) according to one-way ANOVA followed by Tukey's test. Microphotographs of cells after 72h of exposure to PHY, PHY/β-CD and PHY/SB-E-β-CD inclusion complexes and physical mixtures show the reduction of the cell population after treatments**.** The scale (red bar) corresponds to 100 μm (C).

The use of β-CD and modified β-CDs, such as hydroxypropyl-β-CD (HP-β-CD) and SB-E-β-CD, has been extensively described for improving physical-chemical properties and consequently the bioactivity of terpenes. The addition of the hydroxypropyl or sulfobutyl groups to the outer surface of β-CD considerably improves its solubility. In this work, we chose to use SB-E-β-CD to assess whether its polyanionic character could have any additional influence on the complexation of phyllacanthone, since HP-β-CD is neutral just like its natural precursor cyclodextrin (β-CD). Moreover, native and modified CDs, particularly SB-E-βCD, are widely used as excipients in pre-clinical safety studies because of their excellent physicochemical and pharmacological properties and limited/reversible toxicity, particularly when dosed orally (Lima et al., 2016). There is still a significant lack of clinical studies validating their use in humans. We hope that these preliminary results will encourage the use of SB-E-β-CD to enable clinical trials with terpenes such as PHY.

4. Conclusions

In this report, we have demonstrated that the complexation of PHY with β-CD and SB-E-β-CD may be a promising alternative for solving the physicochemical and bioavailability problems of this diterpene. Both inclusion complexes were characterized by FTIR, NMR and microscopic studies. In addition, we determined the mechanism of complexation using an *in silico* approach. Both inclusion complexes preserved the cytotoxic activity of PHY against melanoma cells and exhibited increased dissolution rates, suggesting that the complexation improved PHY aqueous solubility. Altogether, these findings encourage the use of both (natural or chemically modified) CDs as carriers of PHY in pharmaceutical formulations or drug delivery systems as a strategy to improve its stability and ensure better bioavailability *in vivo*.

Authors contributions

CSCA, CAAF and RGOJ contributed to PHY isolation; CSCA, YKSCT, GUMN, VLAS and APO performed complex inclusion preparation and characterization (NMR, FTIR and SEM analyses); CSCA and GUMN performed entrapment efficiency and *in vitro* dissolution studies; LP and RGOJ performed all cytotoxic activity evaluation; CEYL and EBAF performed molecular docking analysis; CSCA, RGOJ and JRGSA participated in the design of manuscript, data analysis and interpretation; JRGSA and RGOJ supervised the entire study.

Conflict of interest

The authors declare no conflict of interest.

Acknowledgments

The authors thank CAPES-FACEPE [88887.615975/2021-00] for financial support, the Franco-Brazilian Network on Natural Products (FB2NP) and CycloLab® for providing Dexolve® (SB-E-β-CD).

REFERENCES

Abril-Sánchez C.A., Matencio A., Navarro-Orcajada S., García-Carmona F., López-Nicolás J.M. (2019). Evaluation of the properties of the essential oil citronellal nanoencapsulated by cyclodextrins. Chemistry and Physics of Lipids, https://doi.org/10.1016/j.chemphyslip.2019.02.001.

Ali S.M., Muzaffar S. (2019). Validating strategy of quantitative ROESY analysis for structure determination of cyclodextrin inclusion complexes. Journal of Molecular Structure, https://doi.org/10.1016/j.molstruc.2018.08.086

Alves C.S.C., Oliveira A.P., Oliveira-Junior R.G., Santos R.F., Santos A.D.C., Tavares G.F., Almeida J.R.G.S. (2019). Caracterização físico-química de complexos de inclusão contendo os monoterpenos cânfora e 1,8-cineol, constituintes majoritários dos óleos essenciais de *Croton conduplicatus*, em β-ciclodextrina. Revista Virtual de Química, DOI: https://doi.org/10.21577/1984-6835.20190030

Bernini A., Spiga O., Ciutti A., Scarselli M., Bottoni G., Mascagni P., Niccolai, N. (2007). NMR studies of the inclusion complex between β-cyclodextrin and paroxetine. European Journal of Pharmaceutical Sciences, https://doi.org/10.1016/j.ejps.2004.04.007.

Brewster M.E., Loftsson T. (2007). Cyclodextrins as pharmaceutical solubilizers. Advanced Drug Delivery Reviews, https://doi.org/10.1016/j.addr.2007.05.012.

Carneiro S.B., Duarte F.I.C., Heimfarth L., Quintans J.S.S., Quintans-Júnior L.J., Veiga-Júnior V.F., Lima A.A.N. (2019). Cyclodextrin-Drug Inclusion Complexes: In Vivo and In Vitro Approaches. International Journal of Molecular Sciences, https://doi.org/10.3390/ijms20030642

Domingues J.S.F., Santos S.M.D., Ferreira J.N.R., Monti B.M., Baggio D.F., Hummig W., Araya E.I., Paula E., Chichorro J.G. (2022). Antinociceptive effects of bupivacaine and its sulfobutylether-β-cyclodextrin inclusion complex in orofacial pain. Naunyn-Schmiedeberg's Archives of Pharmacology, https://doi.org/10.1007/s00210-022-02278-4.

Eid E.E.M., Abdul A.B., Suliman F.E.O., Sukari M.A., Rasedee A., Fatah S.S. (2011). Characterization of the inclusion complex of zerumbone with hydroxypropyl-β-cyclodextrin. Carbohydrate Polymers, https://doi.org/10.1016/j.carbpol.2010.10.033.

Faucci M.T., Melani F., Mura P. (2002). Computer-aided molecular modeling techniques for predicting the stability of drug–cyclodextrin inclusion complexes in aqueous solutions. Chemical Physics Letters, https://doi.org/10.1016/S0009-2614(02)00410-4.

Fenyvesi E., Szemán J., Csabai K., Malanga M., Szente L. (2014). Methyl-beta-cyclodextrins: the role of number and types of substituents in solubilizing power. Journal of Pharmaceutical Sciences, https://doi.org/10.1002/jps.23917.

Fenyvesi E., Vikmon M., Szente L. (2016). Cyclodextrins in food technology and human nutrition: benefits and limitations. Critical Reviews in Food Science and Nutrition, https://doi.org/10.1080/10408398.2013.809513.

Ferraz C.C.A., Oliveira Júnior R.G., Oliveira A.P., Groult H., Beaugeard L., Picot L., Alencar Filho E.B., Almeida J.R.G.S., Nunes X.P. (2020). Complexation with β-cyclodextrin enhances apoptosis-mediated cytotoxic effect of harman in chemoresistant BRAF-mutated melanoma cells. European Journal of Pharmaceutical Sciences, https://doi.org/10.1016/j.ejps.2020.105353.

Gandhi S.R., Quintans J.S.S., Gandhi G.R., Araujo A.A.S., Quintans-Júnior L.J. (2020). The use of cyclodextrin inclusion complexes to improve anticancer drug profiles: a systematic review. Expert Opinion on Drug Delivery, https://doi.org/10.1080/17425247.2020.1776261

Jahed V., Zarrabi A., Bordbar A.K., Hafezi M.S. (2014). NMR (^{1}H, ROESY) spectroscopic and molecular modelling investigations of supramolecular complex of β-cyclodextrin and curcumin. Food Chemistry, https://doi.org/10.1016/j.foodchem.2014.05.094.

Kumar R., Kaur K., Uppal K., Mehta S.K. (2017). Ultrasound processed nanoemulsion: A comparative approach between resveratrol and resveratrol cyclodextrin inclusion

complex to study its binding interactions, antioxidant activity and UV light stability. Ultrasonics Sonochemistry, https://doi.org/10.1016/j.ultsonch.2017.02.004.

Lima P.S., Lucchese A.M., Araújo-Filho H.G., Menezes P.P., Araújo A.A.S., Quintans-Júnior L.J., Quintans J.S.S. (2016). Inclusion of terpenes in cyclodextrins: Preparation, characterization and pharmacological approaches. Carbohydrate Polymers, https://doi.org/10.1016/j.carbpol.2016.06.040

Marques, H.M.C. (2010) A review on cyclodextrin encapsulation of essential oils and volatiles. Flavour and Fragrance Journal, https://doi.org/10.1002/ffj.2019.

Mopac, J.J.P (2016). Stewart, Software is Stewart Computational Chemistry, Colorado Springs, CO.

Morris G.M., Huey R., Lindstrom W., Sanner M.F., Belew R.K., Goodsell D.S., Olson A.J. (2009) Software news and updates AutoDock4 and AutoDockTools4: Automated docking with selective receptor flexibility. Journal of Computational Chemistry, https://doi.org/10.1002/jcc.21256.

Mossman, T. (1983). Rapid colorimetric assay for cellular growth and survival: application to proliferation and cytotoxicity assays. Journal of Immunology Methods, https://doi.org/10.1016/0022-1759(83)90303-4.

Mura, P. (2015). Analytical techniques for characterization of cyclodextrin complexes in the solid state: A review. Journal of Pharmaceutical and Biomedical Analysis, https://doi.org/10.1016/j.jpba.2015.01.058.

Oliveira A.P., Silva A.L.N., Viana L.G.F.C., Silva M.G., Lavor E.M., Oliveira-Júnior R.G., Alencar-Filho E.B., Lima R.S., Mendes R.L., Rolim L.A., Anjos D.S.C., Ferraz L.R.M., Rolim-Neto P.J., Silva M.F.S., Pessoa C.O., Almeida J.R.G.S. (2019). β-Cyclodextrin complex improves the bioavailability and antitumor potential of cirsiliol, a flavone isolated from *Leonotis nepetifolia* (Lamiaceae). Heliyon, https://doi.org/10.1016/j.heliyon.2019.e01692.

Oliveira-Filho R.D., Silva A.R.A.E., Moreira R.A., Nogueira N.A.P. (2018). Biological activities and pharmacological applications of cyclodextrins complexed with essential oils and their volatile components: A systematic review. Current Pharmaceutical Design https://doi.org/ 10.2174/1381612824666181120093634.

Oliveira-Júnior R.G., Ferraz C.A.A., Pontes M.C., Cavalcante N.B., Araújo E.C.C., Oliveira A.P., Picot L., Rolim L.A., Almeida J.R.G.S. (2018). Antibacterial activity of terpenoids isolated from *Cnidoscolus quercifolius* Pohl (Euphorbiaceae), a Brazilian medicinal plant

from Caatinga biome. European Journal of Integrative Medicine, https://doi.org/10.1016/j.eujim.2018.10.011.

Oliveira-Júnior R.G., Ferraz C.A.A., Oliveira A.P., Araújo E.C.C., Prunier G., Beaugeard L., Groult H., Picot L., Alencar Filho E.B., El Aouad N., Rolim L.A., Almeida J.R.G.S. (2022). Bis-nor-diterpene from *Cnidoscolus quercifolius* (Euphorbiaceae) induces tubulin depolymerization-mediated apoptosis in BRAF-mutated melanoma cells. Chemico-Biological Interactions, https://doi.org/10.1016/j.cbi.2022.109849.

Pettersen E.F., Goddard T.D., Huang C.C., Couch G.S., Greenblatt D.M., Meng E.C., Ferrin T.E. (2004). UCSF Chimera - A visualization system for exploratory research and analysis. Journal of Computational Chemistry, https://doi.org/10.1002/jcc.20084.

Riekes M.K., Tagliari M.P., Granada A., Kuminek G., Silva M.A.S., Stulzer H.K. (2010). Enhanced solubility and dissolution rate of amiodarone by complexation with β-cyclodextrin through different methods. Materials Science and Engineering: C, https://doi.org/10.1016/j.msec.2010.05.001.

Santos K.A., Silva E.A, Silva C. (2020). Supercritical CO_2 extraction of favela (*Cnidoscolus quercifolius*) seed oil: Yield, composition, antioxidant activity, and mathematical modeling. The Journal of Supercritical Fluids, https://doi.org/10.1016/j.supflu.2020.104981.

Sapte S., Pore Y. (2016). Inclusion complexes of cefuroxime axetil with β-cyclodextrin: Physicochemical characterization, molecular modeling and effect of L-arginine on complexation. Journal of Pharmaceutical Analysis, https://doi.org/10.1016/j.jpha.2016.03.004.

Srinivasan K., Stalin T. (2014). Study of inclusion complex between 2, 6-dinitrobenzoic acid and β-cyclodextrin by ^{1}H NMR, 2D ^{1}H NMR (ROESY), FT-IR, XRD, SEM and photophysical methods. Spectrochimica Acta Part A: Molecular and Biomolecular Spectroscopy, https://doi.org/10.1016/j.saa.2014.03.106.

Sobrinho T.J.S.P., Tavares E.A., Castro V.T.N.A., Veras-Filho J., Militão G.C.G., Silva T.G., Amorim E.L.C. (2012). Antiproliferative activity of species of the genus *Cnidoscolus* against HT-29, Hep-2 and NCI-H292 cells. 2012. Molecular & Clinical Pharmacology, 3(2) 55-61.

Trott O., Olson A. (2010). Autodock vina: improving the speed and accuracy of docking with a new scoring function, efficient optimization and multithreading. Journal of Computational Chemistry, https://doi.org/10.1002/jcc.21334.

Zhou H.Y., Jiang L.J., Zhang Y.P., Li J.B. (2012). β-Cyclodextrin inclusion complex: preparation, characterization, and its aspirin release *in vitro*. Frontiers of Materials Science, https://doi.org/10.1007/s11706-012-0176-2.